Safe Walking Route Recommender Based on Fall Risk Calculation Using a Digital Human Model on a 3D Map

MAYUKO MINAKATA[1], TSUBASA MARUYAMA [ID]2, MITSUNORI TADA [ID]2, PRIYANKA RAMASAMY[1], SWAGATA DAS [ID]1, AND YUICHI KURITA [ID]1, (Member, IEEE)

[1]Graduate School of Advanced Science and Engineering, Hiroshima University, Higashihiroshima 739-8511, Japan
[2]National Institute of Advanced Industrial Science and Technology, Koto-ku, Tokyo 135-0064, Japan

Corresponding author: Swagata Das (swagatadas@hiroshima-u.ac.jp)

ABSTRACT The recent increase in sedentary lifestyles has highlighted the importance of physical activity in our daily lives. Although fall accidents are a common cause of injuries among the elderly, walking is one of the simplest physical activities available. Therefore, walking route selection and identification of walking behavior in different scenarios remains a widely researched area. This paper is about developing a walking-route recommender system that proposes a safe route to the user and reduces the probability of fall accidents. We determine route candidates after the start and endpoints are fed to the system. Then the tripping risk involved in each route candidate is identified by performing several walking simulations of a digital human model on a three-dimensional laser-scanned point cloud. Finally, a safe route is determined after considering the user's age and the tripping risk. It was confirmed that tripping risk could be competently estimated according to the considered age group.

INDEX TERMS Navigation, fall prevention, tripping risk, walking simulation, digital human model, point cloud.

I. INTRODUCTION

Since "stay home" is recommended worldwide to prevent COVID-19 infection, the physical movement has drastically reduced. Health-care workers and medical experts recommend walking as a critical determinant for alleviating the onset of lifestyle-related diseases. Knowing the value of mobility for a better Quality of Life (QoL) can increase motivation to perform at-home exercises [1]. In Japan, walking has been embraced by individuals of all age groups but is especially popular among those aged 50 years, and the elderly [2]. Walking is a routine exercise, but it is challenging to maintain the motivation for such a time-consuming and monotonous activity. The motivation for walking can be maintained by (a) ensuring an appropriate amount of exercise, (b) alerting users of the beneficial effects of training, and (c) providing a safe route. In a related research (a), Claes *et al.* developed a smartphone platform to present the degree of physical burden during exercise to users [3]. This degree of burden was estimated from acceleration and heart rate data measured through

wearable devices attached to the chest. In another research to promote awareness of training effects (b), Hargreaves *et al.* performed a walking program for 12 weeks. They presented the target number of steps set according to the individual based on the individual's record of past steps [4]. An increase in self-efficacy was observed as the average number of steps per day increased. In another research to support safety assurance (c), Lee *et al.* developed a system to predict falls using a smartphone's acceleration sensor [5]. The importance of ensuring safety (c) is exceptionally high because there are several instances where walking is discontinued due to difficulties after a fall.

Fall risk is affected by the walking environment that involves geographical features and human features, such as exercise capacity. In a research on determining the fall risk in an environment, Curl *et al.* developed a checklist for assessing the road surface for walkability. The checklist items were decided by interviewing older adults in detail where they needed to pay attention while walking and where falling probability was high [6]. In another research on determining fall risk affected by exercise capacity, Begg *et al.* developed a system to display the minimum toe clearance information

The associate editor coordinating the review of this manuscript and approving it for publication was Yin Zhang [ID].

to the user by measuring the foot's trajectory while walking in real-time [7]. These researches presented the fall risk to pedestrians to ensure a safe road and to warn of danger. In this situation, although pedestrians can recognize dangerous locations through the warning system while taking a walk, they are not aware of a safe path where they can walk with a lesser risk of falling.

Currently, no work has been done that recommends a safe route to pedestrians before they begin the activity. Therefore, this paper presents a walking-route recommender system that proposes a safe route with lowered fall risk. We performed the route recommendation based on fall risk calculation. The environment map data of the concerned area is used to determine the recommended route. The fall risk is calculated through an existing tripping risk quantification method using a digital human model on a three-dimensional (3D) laser-scanned point cloud of the walking environment. The remainder of this paper is organized as follows. The Introduction section is followed by Related work, in which a systematic yet brief literature survey is provided. The following section describes the proposed walking route recommendation method based on fall risk calculation. This section is followed by a use case of the proposed method, and the paper is finally concluded.

II. RELATED WORK

In this section, we report recent research advances related to this paper. We divide the literature into four areas: route recommendation systems, fall risk calculation, and Estimation, using 3D maps for navigation and behavior study of pedestrians.

A. ROUTE RECOMMENDATION

Simulation and recommendation of evacuation methods is a type of route recommendation where public spaces are considered [8]. Such types of researches help design evacuation strategies to reduce casualties and damages in the events of natural or man-made disasters. Other researches have highlighted the importance of walking route recommendations for promoting good health [9]. Recent research has proposed an application-based safe route planning solution using COVID-19 occurrence data for cyclists and pedestrians. This study aims at keeping the users away from virus transmission spots [10]. Environmental factors such as air cleanliness [11], land use mix, infrastructure, aesthetics and accessibility [12], transport carbon footprint [13], and post-rain accumulated water [14] and traffic factors [12] such as traffic volume and speed, quality of path surface, and safety level of road crossings have also been made primary factors for route recommendation algorithm design. The Land Use Regression (LUR) model was used to model the concentration of black carbon to be calculated in the route candidates for home-to-school commuting [11]. Other researches have aimed at designing route recommendation algorithms for the specific benefit of Chronic Obstructive Pulmonary Disease (COPD)

patients [15], visually impaired users [16], and Patients with Motor Disabilities (PWMD) [17]. Such researches have given more importance to the customization of the algorithm using user-specific necessities. Gharebaghi *et al.* have proposed a Fuzzy Approach for PWMD user (on manual wheelchair)-specific route recommendation in which the user's confidence while dealing with obstacles such as uneven pavement and slopes is used to personalize the route [17].

B. FALL RISK CALCULATION AND ESTIMATION

Fall risk calculation is another primary aspect considered in this paper. Therefore, we report the recent works that have significantly contributed to this area. Three categories of researches have evolved, namely: reasons contributing to falls, fall prevention strategies, and fall risk factors [18]. Identifying the risk factors that contribute to falls helps us design optimum fall prevention strategies. Jensen *et al.* have categorized these risk factors as extrinsic and intrinsic (health-related) [19]. Extrinsic risk factors include the environmental conditions present in the individual's surroundings, such as clutter, land or floor elevation patterns, loose rugs leading to tripping hazards, lack of railings or grab bars to hold in stairs and bathing areas, and poor lighting. Intrinsic factors include the individual's mental and physical condition. Assessment models such as Home Assessment Profile (HAP) [20], cumulative risk score [21] and FROP-Com (Fall Risk for Older Adults in the Community) [22] were developed for risk calculation by considering the extrinsic factors. A fall risk assessment algorithm for the Japanese inpatient population was proposed recently by considering nine individual intrinsic factors that contribute to increased risk of falls [23]. Fall risk assessment can be done in static and dynamic situations. The intrinsic factors are dynamic since the individual's condition changes as they progress in the environment. Simulation techniques, on the other hand, can predict fall risk in 'what-if' situations [24]. Such simulation is beneficial in evacuation scenarios where environmental factors play a significant role.

C. USING 3D MAPS FOR NAVIGATION

3D digital maps are becoming increasingly on-demand for applications involving smart cities, high-tech living, and autonomous navigation. These are the next step of digital cities, and an essential tool for storing spatial information [25]. 3D maps have been proved to be more beneficial to identify specific intricate locations for pedestrian navigation when compared to 2D maps. Three main supportive aspects that can be delivered better through 3D maps compared to 2D are self-orientation, navigation decision, and the knowledge of spatial information [26]. 3D maps are generally constructed using camera-based approaches. Novel data management and processing methods are also being introduced. Jeong *et al.* proposed odometry estimation for live 3D point cloud registration and error minimization to remove moving vehicles and pedestrians from 3D point clouds using 2D semantic segmentation [27]. These processes

were achieved to ensure low computational time and efficient 3D map construction.

D. BEHAVIOUR STUDY

Studying the behavior of pedestrians in specific environments helps us design more efficient navigation systems tailored to the needs of the users. Environmental features are the most prominent factors that affect pedestrian behavior. Studies have shown that people prefer straight, direct paths rather than zig-zag paths, irrespective of the energy expenditure involved [28]. Additionally, visual environmental features can influence the walking speed of pedestrians. The walking speed was reported lower in spaces with a higher degree of natural characteristics such as greenery. In such spaces, people also tend to find city noises more annoying as compared to less natural spaces [29]. The noises we encounter while walking also significantly affect our walking speed. People increase their walking speed as they hear traffic noises, whereas relaxation sounds such as birdsong relax the individual and lower their walking speed [30]. However, it was also observed that active commuting (biking and walking) is often evaded due to psychosocial and personal barriers rather than environmental barriers [31]. The usage of smartphones can have an impact on a pedestrian's priorities. In a Korean study, smartphone walkers reported safety and route quality as essential for route selection. On the other hand, walkers without smartphones considered distance and positive walking experience to be more critical [32]. Using smartphones during walking has an apparent effect on the walking speed accompanied by distracting behavior [33]. Accessibility and street connectivity were also strongly correlated to walkability in the pedestrian street by Jabbari *et al.*. Here, accessibility was calculated by Angular Segment Analysis by Metric Distance (ASAMeD), and street connectivity was calculated through the space syntax measure of connectivity [34]. An agent-based study showed that landmarks tend to improve the user's correspondence with the navigation routes. Therefore, landmarks play an essential role in route planning and also tend to lead agents towards green areas more frequently [35].

III. WALKING ROUTE RECOMMENDER SYSTEM BASED ON FALL RISK

A. SYSTEM CONFIGURATION

This study proposes a system that recommends safe walking routes. At first, the user inserts the start and endpoints of their route. The system determines multiple routes between the two points. The travel distance and the fall risk by tripping are estimated for each route. Finally, an appropriate and safe walking route is determined for the user based on the fall risk, distance, and user's age. The path structure is acquired from Google Maps, and the roughness present on the surface of the road (which largely determines the fall risk) is acquired from a 3D laser-scanned point cloud of the environment (called 3D map).

Figure 1 shows the walking-route recommender system. The system consists of a tripping risk calculator (A1) and
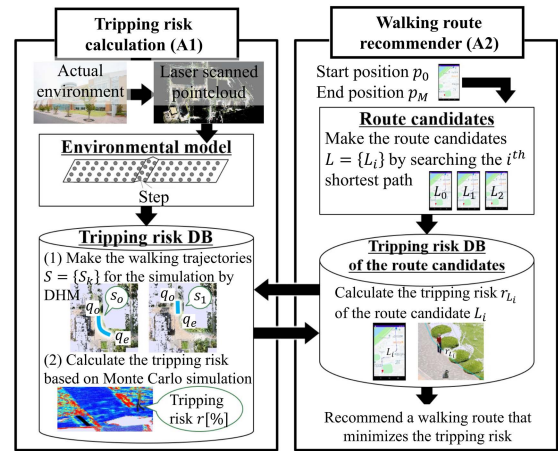

FIGURE 1. System configuration (DB: database).

a recommender (A2). Part (A1) creates the database of the tripping risk by walking simulation on the 3D map [36]. Part (A2) creates a route candidate group from the start to endpoints based on Google Maps and determines the tripping risk along every route candidate using the tripping database. Finally, the route L_a that minimizes the user's tripping risk in their age group is recommended.

B. CALCULATING FALL RISK USING 3D MAPS AND DIGITAL HUMAN MODEL

The tripping risk calculation part (A1) prepares a tripping risk database along each walking route. This database is vital to determine the optimum route that involves the lowest probability of tripping. An existing technique calculates the tripping risk, namely, simulation of the walking situation on a 3D laser-scanned point cloud [36]. Our route recommender system is visualized by a 3D laser-scanned point cloud of the Nihon University campus of Japan. The fall risk calculation method is reported below in further detail.

1) ESTIMATION OF THE WALKING SURFACE AND PATH STRUCTURE FROM THE LASER-SCANNED POINT CLOUD

This method first includes the extraction of a point cloud representing the walking surface [36]. This extraction is done by the popular region-growing method [37]. The path graph illustrating the environment's route connectivity is constructed based on the obtained point cloud distribution. Figure 2 shows the image of an original point cloud and a path graph showing the various route connections of the same point cloud. From this path graph, the walking trajectory from the start point to any target point and the possible walking motions on the 3D point cloud can be simulated [38].

2) SIMULATION WITH THE DIGITAL HUMAN MODEL (DHM)

Walking simulation using the DHM is performed on the actual environment model mentioned in the section III-B1 [39]. The DHM had 41 degrees of freedom, and the dimensions of each segment of the body are based on the gait database [40].
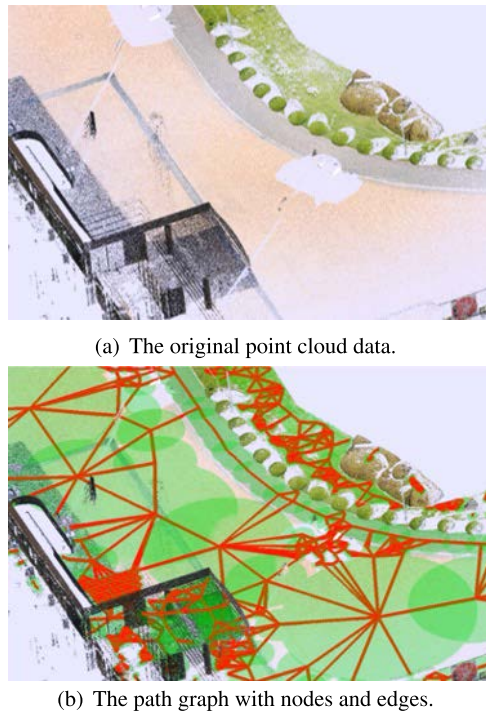
(a) The original point cloud data.

(b) The path graph with nodes and edges.

FIGURE 2. The generated navigation graphs from point cloud data.

FIGURE 3. Conditions for determining tripping risk in simulation.

The simulation is realized in three steps as proposed in [36]. The first step is to select nodes and edges between q_0 and q_e or the start and endpoints, respectively. The second step is to determine the walking trajectory s_k based on an optimization algorithm. The third step simulates the walking motion, i.e., full-body motion during the walking trajectory s_k. The simulation generates the motions of each step referring to the flat-walking motion data captured in the gait database [40] and the walking-related parameters (step length and toe clearance) [41].

3) CALCULATION OF THE TRIPPING RATE

The tripping rate is calculated in a Monte Carlo simulation [42], where the walking simulation is executed many times with different walking parameters [36]. In each trial, occurrences of tripping or non-tripping are estimated by simulating the collision between the DHM foot and the walking surface. The toe clearance C_t is the difference between the current toe height of the DHM and the height of the road surface where the next step will be placed during the walking simulation. Figure 3 shows the foot of the DHM and the road surface for determining the toe clearance C_t in two different situations of safe and *tripping* surfaces. In other words, $C_t \leq 0$ represents the condition when the toes of the swing leg of the DHM model are positioned at a lower height compared to the walking terrain, such that *tripping* probability is high. When the foot of the DHM interferes with the road surface as shown in Figure 3(b), i.e., the condition of $C_t \leq 0$ is encountered, it is judged as tripping.

The number of tripping occurrences C_{trip} in each trial of walking simulation is calculated by Equation 1. The ratio of
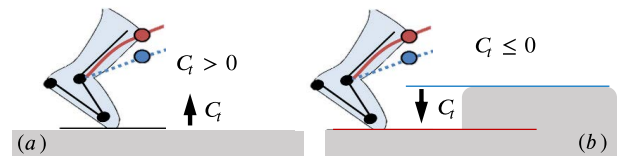
the number of tripping occurrences C_{trip} to the total number of simulations N_{sim} is termed as the tripping rate $r(q_0, q_e)$ while walking from point q_0 to q_e. Therefore, the tripping rate $r(q_0, q_e)$ is given by Equation 2.

$$if \ C_t \ \leq \ 0 \ then \ C_{trip} = C_{trip} + 1 \qquad (1)$$

$$r(q_0, q_e) = \frac{C_{trip}}{N_{sim}} \times 100 \ [\%] \qquad (2)$$

The algorithm described in this section is used to calculate the tripping rate involved in a particular walking trajectory between the start position q_0 to the end position q_e to quantify the fall risk.

C. RECOMMENDATION OF THE OPTIMUM WALKING ROUTE CONSIDERING TRIPPING RISK

Part (A2) of the proposed system refers to the tripping risk database obtained in part (A1) and recommends route candidates to the user, avoiding routes with high tripping risk as shown in Figure 1. A group of route candidates L is generated from the map data (Google Maps).

A route candidate group is termed as $L = \{L_i \mid 0 \leq i \leq N\}$ where L_i is the ith route candidate. The total distance to be walked if the ith route candidate $L_i \in L$ is selected, is represented as $d(L_i)$. The structure of the route candidate group L_i is shown in Figure 4. The ith route candidate consists of relay points p_j between the start point p_0 and the end point p_M such that $p_j \mid 0 \leq j \leq M$. Next, the fall risk $t(L_i)$ along each route L_i is calculated based on the tripping risk data obtained during the step (A1). Finally, a safe route with low tripping risk is recommended as the route L_a that minimizes the tripping risk. The route recommendation method is detailed below.

1) GENERATION OF THE ROUTE CANDIDATE GROUP L

A route candidate group is prepared to compare the fall risk involved in each route. After the user specifies the start and endpoints (p_0 and p_M, respectively) of the walking route, the shortest-route L_0 between p_0 and p_M is determined by the shortest-route search method [43]. Moreover, the Nth shortest path search method [44] generates route candidate groups $L = \{L_i\}$ in the order of decreasing distance $d(L_i)$.

As shown in Figure 5, all relay points of the shortest route are considered as branch point candidates in the Nth shortest path search method [44]. The shortest route search is executed from the start to each branch point and from the branch to the endpoints. The distance covered in each shortest route for all branch points is calculated. The shortest path among these moving distances is finally selected. This process is repeated N times to find the Nth shortest path.
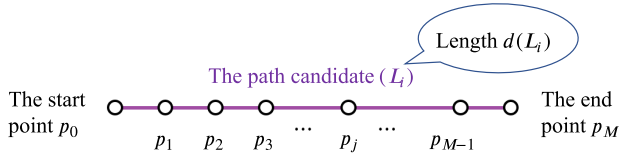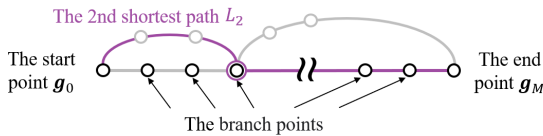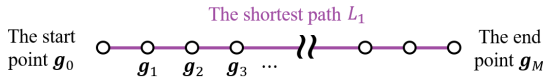
FIGURE 4. Structure of the route candidates.

FIGURE 5. Procedure for determining the Nth shortest path.

2) COORDINATE TRANSFORMATION OF ROUTE CANDIDATES AND WALKING TRAJECTORY

The coordinate system represents the relay points of the route candidates L_i and the walking simulation trajectory s_k in the tripping risk database. The relay points p_j along the route candidates L_i ($L_i \in L$) are expressed by their longitude and latitude in the geographical coordinate system. Alternatively, the start point q_0 and endpoint q_e along the trajectory s_k created in section III-B2 are represented in the Euclidean coordinate system of the point cloud data. Thus, these data are converted to a common rectangular coordinate plane (9 series) [45].

(a) Transformation from geographical coordinates
The geographical coordinate system is converted into a rectangular coordinate plane through a conventional coordinate transformation formula [45]. This helps to express the relay points $\hat{g}_j$ along route L_i in rectangular coordinates.

(b) Transformation of point cloud coordinates
The next step is to construct the coordinate transformation matrix T. Eight landmark points (such as corners) are selected from the 3D map and designated as x_i ($i = 0, 1, 2, \ldots, 7$). The corresponding eight points y_i ($i = 0, 1, 2, \ldots, 7$) on the rectangular plane are also manually selected from Google Maps. Now the X and Y coordinates are designated as $X = [x_0, x_1, x_2, \ldots, x_7]$, $Y = [y_0, y_1, y_2, \ldots, y_7]$. A coordinate transformation matrix T is calculated from x_i to y_i to satisfy $y_i = Tx_i$. Using the obtained matrix T, the coordinates of the start $\hat{q}_0$ and the end points $\hat{q}_e$ of the walking trajectory s_k are expressed in the rectangular plane coordinate system as follows:

$$[\hat{q}_0, \hat{q}_e] = T \times [q_0, q_e] \tag{3}$$

This coordinate transformation gives the route candidate $L = \{L_i'\}$ ($L_i' = \{\hat{p}_j\}$), and the walking simulation trajectory
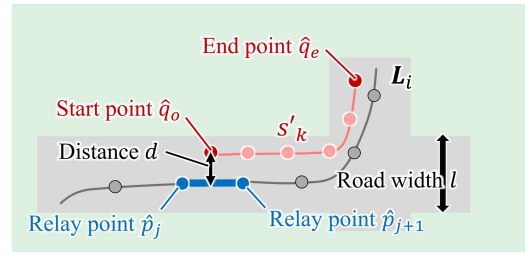

FIGURE 6. The positional relationship of $\hat{p}_j, \hat{p}_{j+1}, \hat{q}_0, \hat{q}_e$.
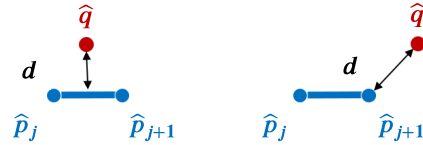

FIGURE 7. Condition to calculate the distance (d).

group $S = \{s_k' \mid 0 < k < N_s\}$ in the rectangular plane coordinate system is also obtained. Each walking simulation trajectory can be represented as $s_k' = \{\hat{q}_l \mid 0 \le l \le e\}$.

3) DETERMINING THE WALKING TRAJECTORY s_k' BELONGING TO THE ROUTE L_i'

The walking trajectories s_k' belonging to each route candidate L_i' are searched from the walking trajectory group $S = \{s_k'\}$ of the tripping risk database. As shown in Figure 6, the start and end points of the walking trajectory s_k' are set to $\hat{q}_0$ and $\hat{q}_e$, respectively, and the relay points of the routes are set to $\hat{p}_j$. After ensuring that $\hat{q}, \hat{p}_j$, and $\hat{p}_{j+1}$ satisfy Equations 4 and 5, the distance d between the line segment connecting $\hat{p}_j, \hat{p}_{j+1}$ and the point $\hat{q}_0$ or $\hat{q}_e$ is calculated by Equation 6. In Equation 6, n is the normal vector of the line segment connecting $\hat{p}_j, \hat{p}_{j+1}$ and the point on the walking trajectory s_k' ($\hat{q}_0$ or $\hat{q}_e$).

$$(\hat{p}_{j+1} - \hat{p}_j) \cdot (\hat{q} - \hat{p}_j) > 0 \tag{4}$$

$$\| \hat{q} - \hat{p}_j \| < \| \hat{p}_{j+1} - \hat{p}_j \| \tag{5}$$

$$d(q, p_j, p_{j+1}) = \frac{\| (\hat{q} - \hat{p}_j) \cdot n \|}{\| n \|} \tag{6}$$

As shown in Figure 7, Equations 4 and 5 are satisfied when the foot of the perpendicular line from the point $\hat{q}$ to the line segment connecting $\hat{p}_j$ and $\hat{p}_{j+1}$ coincide with the line segment itself. When the distance d from route L_i' is less than or equal to the threshold l for points $\hat{q}_0$ and $\hat{q}_e$, then trajectory s_k' belongs to L_i' as shown in Equation 7.

$$d(\hat{q}_0, \hat{p}_j, \hat{p}_{j+1}) \le l \ \wedge \ d(\hat{q}_e, \hat{p}_j, \hat{p}_{j+1}) \le l \tag{7}$$

The walking trajectory s_k' belonging to the route L_i' is defined as a walking trajectory group $s_{L_i'} = \{s_k'\}$.

4) CALCULATION OF THE FALL RISK

The tripping rate $r(\hat{q}_0, \hat{q}_e)$ is obtained from the tripping risk database created in section III-B by specifying the walking trajectories $s_{L_i'}$ on the route L_i' and the user's age (younger or elderly people). The largest value among the tripping rates

Condition		Coordinate	
		Latitude [°]	Longitude [°]
1	p_0:	37.36185	140.38224
	p_M:	37.35762	140.38053
2	p_0:	37.36184	140.38224
	p_M:	37.35958	140.38035
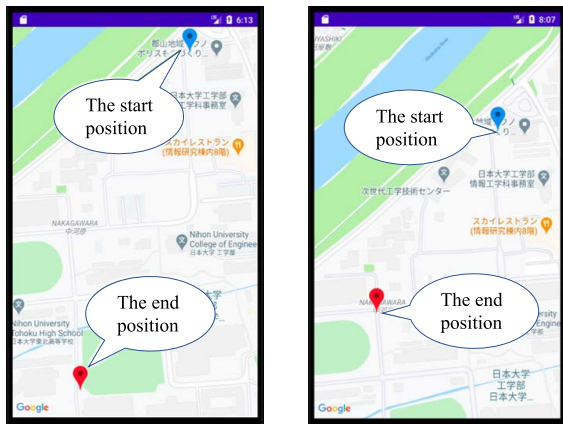
(a) Condition 1	(b) Condition 2

FIGURE 8. The positions of the start and end points.

$\{r(\hat{q}_0, \hat{q}_e)|s'_k \in L'_i\}(\hat{q}_0, \hat{q}_e \in s'_k)$ of the walking trajectory group $L'_i = \{s'_k\}$ is considered as the tripping risk $t(L'_i)$ of the particular route L'_i. The fall risk is averaged for each age group of users (younger or elderly people) to determine the tripping rate corresponding to the age group.

5) DETERMINING THE RECOMMENDED ROUTE L_a

Finally, the recommended walking route L_a that minimizes the fall risk among the route candidate groups L'_i is determined, where t is the calculated fall risk in the route candidate group L'_i as mentioned in section III-C4.

$$L_a = \arg\min_{L'_i \in L} \{t(L'_i)\} \tag{8}$$

IV. CASE STUDY FOR VALIDATING THE PROPOSED METHOD

A. CONDITION

The walking simulation for calculating the fall risk was performed using the DHM and a 3D laser-scanned point cloud of the environment. The conditions and results are described in this section.

1) SELECTION OF THE START AND END POSITIONS

The first step is to input the start p_0 and end p_M positions of the desired walking route and the user's age. The two pairs of start and end positions selected for this case study are shown in Table 1 and Figure 8. The optimum route L_a was recommended for both young and older adults in each condition. An extensive route search follows this.

2) POINT CLOUD DATA FOR CALCULATING THE FALL RISK

A 3D laser-scanned point cloud published by Nihon University was used for calculating the tripping probability. This
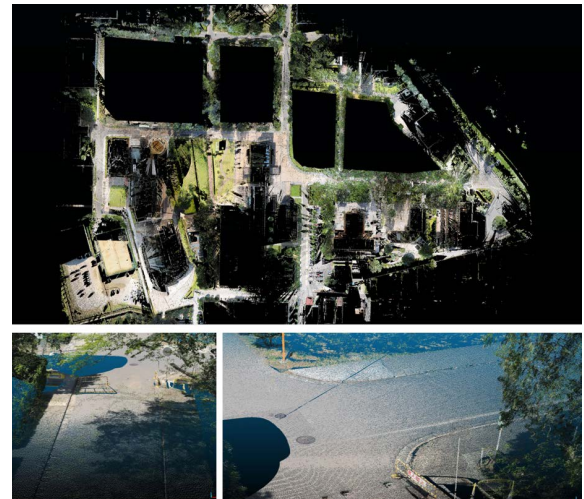

FIGURE 9. The point cloud data.

point cloud was measured by a ground-based laser scanner RIEGL V2-6000 by Nihon University in August 2020. They measured it at 63 places in the engineering faculty of the campus. These individual point cloud data were combined as one-point cloud data to calculate the tripping rate after calibration. The point cloud data used is shown in Figure 9. The total number of points after the combination into a single point cloud were 104, 903, 184 points (600 × 400 m).

3) DHM FOR SIMULATION

The walking simulation for calculating the fall risk was performed using a DHM [40] under the conditions shown in Table 2. The motion capture data of seven young and seven older adults were used for the simulation. The walking simulation was repeated 500 times in the Monte Carlo simulation for each subject. The walking parameters, swing ankle height displacement, and the walking stride are updated based on age-dependent statistics distributions during the Monte Carlo simulation. The tripping rate was calculated with $N = 3500$ (7*subjects* ∗ 500) simulations for each young and elderly group. The parameter settings of sub. 1–7 correspond to the DHM of a young person, whereas those in sub. 8–14 correspond to the DHM of an elderly individual. To represent the route recommendation mathematically, considering 57 pairs of manually specified start q_0 and end points q_e, the system generates the walking trajectory group $S = \{s(q_{0,i}, mq_{e,i})\}(i \in [1, 57])$ to simulate the walking motion by DHM on each trajectory. The tripping rate is calculated for the young (sub. 1–7 in Table 2) and the elderly (sub. 8–14 in Table 3) people separately. Given the walking trajectory $s(q_{0,i}, q_{e,i})$ and the age group A, we could obtain the tripping rate $r_A(q_{0,i}, q_{e,i})$ on the specific walking trajectory.

B. RESULT

This section shows the results of the proposed walking route recommendation system. Figure 10 shows a walking simulation using the reported DHM. The calculation results of the routes and their fall risk are shown in Figures 11 and 12.

TABLE 2. DHMs for walking simulation.

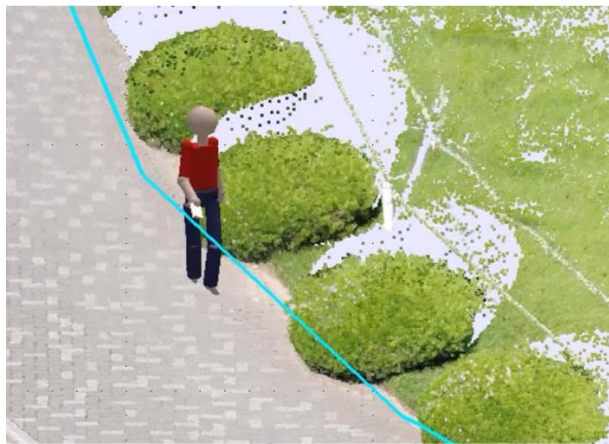| DHM	Gender	Age	Height [cm]	Weight [kg]
Sub.1	Female	13	160.9	49
Sub.2	Female	22	155.7	51
Sub.3	Female	23	155.4	47
Sub.4	Male	21	170.0	124
Sub.5	Male	22	173.2	62
Sub.6	Male	23	175.9	54
Sub.7	Male	24	175.0	70
Sub.8	Female	64	149.6	63
Sub.9	Female	71	155.7	44
Sub.10	Female	71	157.1	63
Sub.11	Male	72	156.1	49
Sub.12	Male	70	167.6	74
Sub.13	Male	71	158.7	74
Sub.14	Male	72	166.0	55

FIGURE 10. A walking simulation representing a DHM in the point cloud.

TABLE 3. The result of fall risk in condition 1.

Route L_i	Distance $d(L_i)$ [m]	Age	Fall risk r [%]
L_0	406.8	Younger	34.4
		Older	49.9
L_1	411.4	Younger	2.2
		Older	4.4
L_2	516.8	Younger	4.4
		Older	9.6

FIGURE 11. The result of the recommended route in condition 1.

TABLE 4. The result of fall risk in condition 2.

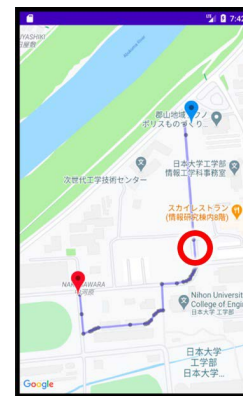| Route L_i	Distance $d(L_i)$ [m]	Age	Fall risk r [%]
L_0	406.8	Younger	12.8
		Older	24.2
L_1	411.4	Younger	27.7
		Older	50.6
L_2	516.8	Younger	41.3
		Older	51.4

The points with the highest fall risk are marked by a red circle in Figures 11 and 12. Tables 3 and 4 represent the distance $d(L_i)$ and the estimated fall risk r for each route L_i and age group. Hence, the safest route for young and older adults can be reported as $L_a = L_1$ in condition 1 and $L_a = L_0$ in condition 2.

C. DISCUSSION

As shown in Tables 3 and 4, the recommended route can minimize the fall risk r of both young and elderly people were $L_a = L_1$ in condition 1, and $L_a = L_0$ in condition 2. It has been reported in previous studies that routes that include steps of height 50 mm have an average fall risk of 23 % for young people and 30% for elderly [36]. The fall risks of routes L_1 and L_2 exceeded 23 % for people of both age groups in condition 2, and both routes included occurrences of step height exceeding 50 mm. Hence, it can be said that our proposed fall risk calculation method is reliable.

Comparing the fall risk by age group in the same route L_i, the fall risk during walking increases with age as shown in Tables 3 and 4. In Japan, people aged fifty and above are approximately seven times more likely to trip than people in their twenties [46]. This trend was mirrored in the calculated tripping risks r. We entered the age group (young or elderly) of each subject to the database for identifying the differences in the tripping risk between young and elderly subjects. The simulation results using the 14-subject database clearly show the difference in the fall risk between the two age groups. This indicates that the DHMs of the young and elderly subjects clearly made a unique impact on the fall risk.

The recommended routes for conditions 1 and 2 were L_1 and L_0, respectively. In condition 1, the fall risk of L_1 was 2.2 % for young and 4.4 % for elderly subjects. The route with the lowest fall risk was recommended because routes with very high and low fall risks were included in the route candidates. However, suppose the user gives preference to
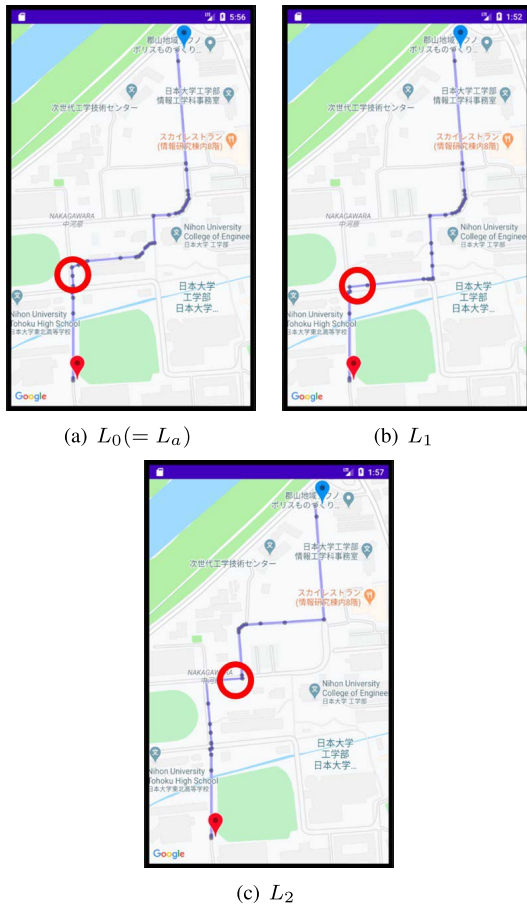
(a) $L_0 (= L_a)$ (b) L_1

(c) L_2

FIGURE 12. The result of the recommended route in condition 2.

FIGURE 13. An example point showing high tripping risk.

(a) Condition 1

(b) Condition 2

FIGURE 14. The difference in tripping risk between the elderly and younger subjects.
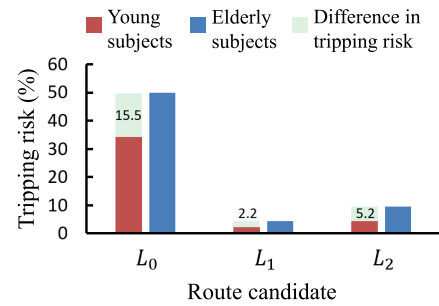
long-distance coverage for their walk. In that case, the recommender system can select moderate fall risk and more extended distance coverage, which makes L_2 as the optimum selection for condition 1. For condition 2, the fall risk of L_0 was 12.8 % for young and 24.2 % for elderly subjects. The route with the lowest fall risk was selected. Unlike condition 1, in the case of condition 2, all other route candidates show high fall risk, especially for the elderly. Therefore, the best route recommendation is L_0, no matter the distance preferences.

In condition 1, if we observe the locations projecting the most significant fall risks (marked with a red circle in Figure 11), routes L_0 and L_2 included both curbs and road bumps or unevenness (see Figure 13), and ditches immediately before the curb. The fall risk was higher at these sites than along L_1 because the step height was relatively large. Therefore, it was confirmed that routes L_0 and L_2 with an estimated high fall risk were avoided, while the safest route L_1 was proposed to the user.
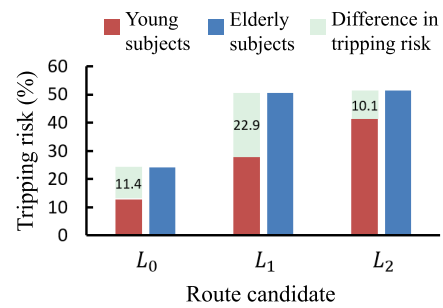
Figure 14 shows the difference in fall risk between the young and the elderly from Tables 3 and 4. In condition 2, the difference in fall risk was 11.4 % for L_0, 22.9 % for L_1, and 10.1 % for L_2. Although the recommended routes for the young and elderly subjects were the same in the case study results reported in this paper, routes with significantly

different fall risks for the young and the elderly subjects were confirmed. In route L_1, older adults' fall risk was significantly higher than young people compared with other routes. Although L_1 can be recommended for young people because the fall risk is low, it should not be recommended for older adults because of high fall risk, thus, an unsafe route. The efficiency of route selection can be further improved by adopting a route such as L_1, as the youth route candidate. In the case of older adults, excluding such routes from the candidate routes group would prevent dangerous route recommendations. A safer and more age-appropriate route can be proposed by choosing the route based on the fall risk linked to each age group and the distance covered.

Furthermore, suppose an individual (preferably young) is looking for a challenging activity, apart from fall-risk reduction. In that case, the proposed methodology can escalate

motivation to exercise by recommending challenging routes to strengthen the user's body functionality. In the future, we aim at performing route recommendations considering the user's physical ability irrespective of age by evaluating the user's ability through pre-tests and measurements. In addition, the route's safety can be evaluated more realistically by adding indices such as the existence of stairs, road surface conditions, post-rain water accumulation, presence of a pedestrian crowd, adequate brightness, and collision probability with vehicle traffic. In terms of tripping risk calculation, in real situations, pedestrians tend to fall due to tripping and tend to lose balance due to other terrain features, such as step down and uneven surfaces. The current version of the recommender system focuses only on the calculation of tripping risk by identifying the probability of collision between the toes of the swing leg and walking terrain surface. However, future work will cover additional factors associated with falling risk, such as losing balance due to uneven walking terrain and stepping down situations.

V. CONCLUSION

This paper proposed a walking route recommender system to support pedestrians. We confirmed that the system could propose a safe route by calculating the tripping rate through walking simulation of a DHM on a 3D laser-scanned point cloud. The system could also propose an age-appropriate route by calculating the tripping risk according to the age group.

REFERENCES

[1] D. Uritani, D. Matsumoto, Y. Asano, and M. Shima, "Relationships between the Short and long-term changes in exercise habit and body composition, blood pressure and health-related quality of life among health program participants," *J. Phys. Therapy Sci.*, vol. 25, no. 4, pp. 521–525, 2013.

[2] T. Tsuji, Y. Sasaki, Y. Matsuyama, Y. Sato, J. Aida, K. Kondo, and I. Kawachi, "Reducing depressive symptoms after the great east Japan earthquake in older survivors through group exercise participation and regular walking: A prospective observational study," *BMJ Open*, vol. 7, no. 3, 2017, Art. no. e013706.

[3] J. Claes, R. Buys, A. Avila, D. Finlay, A. Kennedy, D. Guldenring, W. Budts, and V. Cornelissen, "Validity of heart rate measurements by the garmin forerunner 225 at different walking intensities," *J. Med. Eng. Technol.*, vol. 41, no. 6, pp. 480–485, 2017.

[4] E. A. Hargreaves, N. Mutrie, and J. D. Fleming, "A web-based intervention to encourage walking (StepWise): Pilot randomized controlled trial," *JMIR Res. Protocols*, vol. 5, no. 1, p. e14, Jan. 2016.

[5] Y. Lee, H. Yeh, K.-H. Kim, and O. Choi, "A real-time fall detection system based on the acceleration sensor of smartphone," *Int. J. Control Autom.*, vol. 10, no. 1, pp. 315–326, Jan. 2017.

[6] A. Curl, C. Ward Thompson, P. Aspinall, and M. Ormerod, "Developing an audit checklist to assess outdoor falls risk," *Proc. Inst. Civil Eng.-Urban Des. Planning*, vol. 169, no. 3, pp. 138–153, Jun. 2016.

[7] R. K. Begg, O. Tirosh, C. M. Said, W. A. Sparrow, N. Steinberg, P. Levinger, and M. P. Galea, "Gait training with real-time augmented toe-ground clearance information decreases tripping risk in older adults and a person with chronic stroke," *Frontiers Hum. Neurosci.*, vol. 8, p. 243, May 2014.

[8] J. Zhou, Y. Guo, S. Dong, M. Zhang, and T. Mao, "Simulation of pedestrian evacuation route choice using social force model in large-scale public space: Comparison of five evacuation strategies," *PLoS ONE*, vol. 14, no. 9, Sep. 2019, Art. no. e0221872.

[9] W. Sasaki and Y. Takama, "Walking route recommender system considering SAW criteria," in *Proc. Conf. Technol. Appl. Artif. Intell.*, Dec. 2013, pp. 246–251.

[10] S. Mishra, N. Singh, and D. Bhattacharya, "Application-based COVID-19 micro-mobility solution for safe and smart navigation in pandemics," *ISPRS Int. J. Geo-Inf.*, vol. 10, no. 8, p. 571, Aug. 2021.

[11] L. Boniardi, E. Dons, L. Campo, M. V. Poppel, L. I. Panis, and S. Fustinoni, "Is a land use regression model capable of predicting the cleanest route to school? *Environments*, vol. 6, no. 8, p. 90, 2019.

[12] M. L. Rahman, A. Moore, M. Smith, J. Lieswyn, and S. Mandic, "A conceptual framework for modelling safe walking and cycling routes to high schools," *Int. J. Environ. Res. Public Health*, vol. 17, no. 9, p. 3318, May 2020.

[13] A. Namoun, A. Tufail, N. Mehandjiev, A. Alrehaili, J. Akhlaghinia, and E. Peytchev, "An Eco-friendly multimodal route guidance system for urban areas using multi-agent technology," *Appl. Sci.*, vol. 11, no. 5, p. 2057, Feb. 2021.

[14] T. Opach, C. Navarra, J. K. Rød, and T.-S. Neset, "Pedestrian routing and perspectives: WayFinder's route down the lane—Come on with the rain," *ISPRS Int. J. Geo-Inf.*, vol. 10, no. 6, p. 365, May 2021.

[15] A. Arbillaga-Etxarri, J. Torrent-Pallicer, E. Gimeno-Santos, A. Barberan-Garcia, A. Delgado, E. Balcells, D. A. Rodríguez, J. Vilaró, P. Vall-Casas, A. Irurtia, and R. Rodriguez-Roisin, "Validation of walking trails for the urban TrainingTM of chronic obstructive pulmonary disease patients," *PLoS ONE*, vol. 11, no. 1, Jan. 2016, Art. no. e0146705.

[16] Y. Kajiwara and H. Kimura, "Object identification and safe route recommendation based on human flow for the visually impaired," *Sensors*, vol. 19, no. 24, p. 5343, Dec. 2019.

[17] A. Gharebaghi, M.-A. Mostafavi, G. Edwards, and P. Fougeyrollas, "User-specific route planning for people with motor disabilities: A fuzzy approach," *ISPRS Int. J. Geo-Inf.*, vol. 10, no. 2, p. 65, Feb. 2021.

[18] X. Du, Y. Chen, A. Bouferguene, and M. Al-Hussein, "An agent-based simulation framework for analysing fall risk among older adults in the evacuation procedures," *Saf. Sci.*, vol. 129, Sep. 2020, Art. no. 104790.

[19] J. Jensen, L. Nyberg, Y. Gustafson, and L. Lundin-Olsson, "Fall and injury prevention in residential care–effects in residents with higher and lower levels of cognition," *J. Amer. Geriatrics Soc.*, vol. 51, no. 5, pp. 627–635, 2003.

[20] J. M. Chandler, P. W. Duncan, D. K. Weiner, and S. A. Studenski, "Special feature: The home assessment profile—A reliable and valid assessment tool," *Topics Geriatric Rehabil.*, vol. 16, no. 3, pp. 77–88, 2001.

[21] P. Dargent-Molina, M. N. Douchin, C. Cormier, P. J. Meunier, and G. Bréart, "Use of clinical risk factors in elderly women with low bone mineral density to identify women at higher risk of hip fracture: The EPIDOS prospective study," *Osteoporosis Int.*, vol. 13, no. 7, pp. 593–599, Jul. 2002.

[22] M. Mascarenhas, K. D. Hill, A. Barker, and E. Burton, "Validity of the falls risk for older people in the community (FROP-Com) tool to predict falls and fall injuries for older people presenting to the emergency department after falling," *Eur. J. Ageing*, vol. 16, no. 3, pp. 377–386, Sep. 2019.

[23] T. Nakanishi, T. Ikeda, T. Nakamura, Y. Yamanouchi, A. Chikamoto, and K. Usuku, "Development of an algorithm for assessing fall risk in a Japanese inpatient population," *Sci. Rep.*, vol. 11, no. 1, Dec. 2021, Art. no. 17993.

[24] T. Gräne-Yanoff and P. Weirich, "The philosophy and epistemology of simulation: A review," *Simul. Gaming*, vol. 41, no. 1, pp. 20–50, Feb. 2010.

[25] Z. Zhongyuan, "Research on 3D digital map system and key technology," *Proc. Environ. Sci.*, vol. 12, pp. 514–520, Oct. 2012.

[26] T. Aditya, D. Laksono, H. Sutanta, N. Izzahudin, and F. Susanta, "A usability evaluation of a 3D map display for pedestrian navigation," *Int. Arch. Photogramm., Remote Sens. Spatial Inf. Sci.*, vols. 10, pp. 3–10, Sep. 2018.

[27] J. Jeong, T. S. Yoon, and J. B. Park, "Towards a meaningful 3D map using a 3D Lidar and a camera," *Sensors*, vol. 18, no. 8, p. 2571, 2018.

[28] S. A. Linkenauger, V. Weser, and D. R. Proffitt, "Choosing efficient actions: Deciding where to walk," *PLoS ONE*, vol. 14, no. 9, Sep. 2019, Art. no. e0219729.

[29] M. Franák and L. Režný, "Environmental features influence walking speed: The effect of urban greenery," *Land*, vol. 10, no. 5, p. 459, Apr. 2021.

[30] M. Franák, L. Režný, D. Šefara, and J. Cabal, "Effect of traffic noise and relaxations sounds on pedestrian walking speed," *Int. J. Environ. Res. Public Health*, vol. 15, no. 4, p. 752, Apr. 2018.

[31] A. Castillo-Paredes, N. Inostroza Jiménez, M. Parra-Saldías, X. Palma-Leal, J. L. Felipe, I. Págola Aldazabal, X. Díaz-Martínez, and F. Rodríguez-Rodríguez, "Environmental and psychosocial barriers affect the active commuting to university in Chilean students," *Int. J. Environ. Res. Public Health*, vol. 18, no. 4, p. 1818, Feb. 2021.

[32] J. Lee and M. M. Shepley, "College campuses and student walkability: Assessing the impact of smartphone use on student perception and evaluation of urban campus routes," *Sustainability*, vol. 12, no. 23, p. 9986, Nov. 2020.

[33] C. Gruden and M. Šraml, "Safety analysis of young pedestrian behavior at signalized intersections: An eye-tracking study," *Sustainability*, vol. 13, no. 8, p. 4419, Apr. 2021.

[34] M. Jabbari, F. Fonseca, and R. Ramos, "Accessibility and connectivity criteria for assessing walkability: An application in qazvin, Iran," *Sustainability*, vol. 13, no. 7, p. 3648, Mar. 2021.

[35] G. Filomena and J. A. Verstegen, "Modelling the effect of landmarks on pedestrian dynamics in urban environments," *Comput., Environ. Urban Syst.*, vol. 86, Mar. 2021, Art. no. 101573.

[36] T. Maruyama, S. Kanai, and H. Date, "Tripping risk evaluation system based on human behavior simulation in laser-scanned 3D as-is environments," *Autom. Construct.*, vol. 85, pp. 193–208, Jan. 2018.

[37] R. Adams and L. Bischof, "Seeded region growing," *IEEE Trans. Pattern Anal. Mach. Intell.*, vol. 16, no. 6, pp. 641–647, Jun. 1994.

[38] T. Maruyama, S. Kanai, and H. Date, "Simulating a walk of digital human model directly in massive 3D laser-scanned point cloud of indoor environments," in *Proc. Int. Conf. Digit. Hum. Modeling Appl. Health, Saf., Ergonom. Risk Manage.* Berlin, Germany: Springer, 2013, pp. 366–375.

[39] T. Maruyama, S. Kanai, H. Date, and M. Tada, "Simulation-based evaluation of ease of wayfinding using digital human and as-is environment models," *ISPRS Int. J. Geo-Information*, vol. 6, no. 9, p. 267, Aug. 2017.

[40] Y. Kobayashi, N. Hida, K. Nakajima, M. Fujimoto, and M. Mochimaru. (2019). *Aist Gait Database*. Accessed: Oct. 4, 2021. [Online]. Available: https://unit.aist.go.jp/harc/ExPART/GDB2019.html

[41] T. Maruyama, S. Kanai, H. Date, and M. Tada, "Motion-capture-based walking simulation of digital human adapted to laser-scanned 3D as-is environments for accessibility evaluation," *J. Comput. Design Eng.*, vol. 3, no. 3, pp. 250–265, Jul. 2016.

[42] J. Hammersley, "Monte Carlo methods," in *Monographs on Statistics and Applied Probability*. Springer, Mar. 2013.

[43] E. W. Dijkstra, "A note on two problems in connexion with graphs," *Numer. Math.*, vol. 1, no. 1, pp. 269–271, Dec. 1959.

[44] W. Hoffman and R. Pavley, "A method for the solution of the Nth best path problem," *J. ACM*, vol. 6, no. 4, pp. 506–514, Oct. 1959.

[45] R. Burtch, "A comparison of methods used in rectangular to geodetic coordinate transformations," in *Proc. Amer. Congr. Surv. Mapping (ACSM)*, 2006.

[46] (2020). *Japan's Population Falls for Ninth Straight Year*. Accessed: Feb. 1, 2021. [Online]. Available: https://www.nippon.com/en/japan-data/h00705/

MAYUKO MINAKATA received the B.E. and M.E. degrees from the Biological Systems Engineering Laboratory, Hiroshima University, in 2019 and 2021, respectively. Her research interests include human augmentation, recommender systems, smart coaching, and human modeling.

TSUBASA MARUYAMA received the M.S. and Ph.D. degrees from Hokkaido University, Japan, in 2014 and 2017, respectively. In 2017, he joined the National Institute of Advanced Industrial Science and Technology (AIST), Japan. His research interests include motion measurements, digital twin, and 3D environmental modeling.

MITSUNORI TADA received the M.S. degree from the University of Tokyo, in 1999, and the Ph.D. degree from the Nara Institute of Science and Technology, in 2002. In 2002, he joined the National Institute of Advanced Industrial Science and Technology (AIST), Japan. His research interests include real-time measurement and analysis of human motion for incorporating human factors into cyber-physical systems.

PRIYANKA RAMASAMY received the B.E. degree in electronics and communication engineering from the R.V.S. Faculty of Engineering, affiliated to Anna University, India, in 2014, and the M.E. degree in system cybernetics from the Biological Systems Laboratory, Hiroshima University, in 2021, where she is currently pursuing the Ph.D. degree in system cybernetics with the TAOYAKA Program, under the supervision of Prof. Y. Kurita. Her research interests include machine–human interaction through gamification, physical rehabilitation, human augmentation through soft robotics, and learning of physical and psychological effects through wearable assistive technologies.

SWAGATA DAS received the B.Tech. degree in electronics and communication engineering from the North Eastern Regional Institute of Science and Technology, India, in 2013, the M.Tech. degree in electronics design and technology from Tezpur University, India, in 2015, the M.E. degree in system cybernetics from the TAOYAKA Program, Hiroshima University, in 2018, and the Ph.D. degree in soft robotics from the Biological Systems Engineering Laboratory, Hiroshima University, in September 2020, under the supervision of Prof. Y. Kurita. Since October 2020, she has been appointed as an Assistant Professor at Hiroshima University by Special Appointment in the Project "Smart society for enjoying long healthy life—developing A.I. smart coaching technology that facilitates voluntary skill-up for elderlies." Her research interests include soft and wearable robotics, gamification of rehabilitation, human activity sensing, psychological effects of assistive technologies, and computer vision.
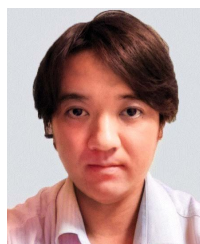
YUICHI KURITA (Member, IEEE) received the B.E. degree from Osaka University, in 2000, and the M.E. and Ph.D. degrees in information science from the Nara Institute of Science and Technology (NAIST), Japan, in 2002 and 2004, respectively. From 2005 to 2007, he was a Research Associate with the Graduate School of Engineering, Hiroshima University, Japan. From 2007 to 2011, he was an Assistant Professor with the Graduate School of Information Science, NAIST. From 2010 to 2011, he was a Visiting Scholar with the School of Mechanical Engineering, Georgia Institute of Technology, USA. Since 2011, he has been with the Graduate School of Engineering, Hiroshima University, as an Associate Professor, and has been a Professor, since 2018. He also works as the Assistant to President by Special Appointment and the Director of the Applied Human Augmentation Project Research Center, Hiroshima University. His research interests include human augmentation, haptics, and human–robot interaction.

. . .